

Evidence in favor of Single Parton Scattering mechanism in Υ and D associated production at the LHC

A.V.Karpishkov,^{*} M.A. Nefedov,[†] and V.A.Saleev[‡]

Samara National Research University,

Moskovskoe Shosse, 34, 443086, Samara, Russia

Abstract

Associated production of prompt $\Upsilon(1S)$ and $D^{+,0}$ mesons has been proposed as a golden channel for the search of Double Parton Scattering, because Single Parton Scattering contribution to the cross-section is believed to be negligible on a basis of leading order calculations in the Collinear Parton Model. We study this process in the leading order approximation of the Parton Reggeization Approach. Hadronization of $b\bar{b}$ -pair into bottomonium states is described within framework of the NRQCD-factorization approach while production of D mesons is described in the fragmentation model with scale-dependent fragmentation functions. We have found good agreement with LHCb data for various normalized differential distributions, except for the case of spectra on azimuthal angle differences at the small $\Delta\varphi$ values. Crucially, the total cross-section in our Single Parton Scattering model accounts for more than one half of observed cross-section, thus dramatically shrinking the room for Double Parton Scattering mechanism.

PACS numbers: 12.38.-t.

^{*}Electronic address: karpishkoff@gmail.com

[†]Electronic address: nefedovma@gmail.com

[‡]Electronic address: saleev@samsu.ru

I. INTRODUCTION

Double Parton Scattering (DPS) mechanism attracts a lot of attention, both theoretically and experimentally. Recent advances in theory of DPS include computation [1] of NLO corrections to $1 \rightarrow 2$ splitting functions, contributing to the scale-evolution of two-parton collinear Parton Distribution Functions (PDFs) and filling remaining gaps in the proof of TMD-factorization theorem for double Drell-Yan process [2].

While for single-scale observables, such as total inclusive cross-section of some hard process with hard scale Q , the DPS contribution is always suppressed by powers of Λ^2/Q^2 , where Λ is some typical hadronic scale, the DPS contribution can be comparable with Single Parton Scattering contribution for the differential distributions in some regions of phase space [3]. In the DPS picture, longitudinal and transverse-momentum correlations of small- x partons, participating in two independent hard scatterings, are quickly washed-out by effects of scale evolution of two-parton PDFs [4], so that double parton PDF effectively factorizes into a product of usual PDFs, leading to the “pocket-formula” description of DPS as:

$$\sigma_{\text{DPS}} \simeq \frac{\sigma_{\text{SPS}}^{(1)} \times \sigma_{\text{SPS}}^{(2)}}{\sigma_{\text{eff}}}, \quad (1)$$

where σ_{DPS} is the DPS contribution to the production cross-section of the pair of objects, $\sigma_{\text{SPS}}^{(1,2)}$ is the Single Parton Scattering (SPS) cross-section of the production of one final-state object and σ_{eff} is the non-perturbative “effective cross-section” which is typically assumed to be universal, energy-independent parameter. Eq. (1) leads to flat distributions for observables correlating momenta of particles produced in independent hard scatterings, in particular, for the azimuthal angle $\Delta\varphi$ or rapidity difference Δy between momenta of components of the pair. In contrast, the SPS contribution to differential distributions in the processes of pair-production of jets, vector bosons or mesons containing heavy flavors, typically decreases rather steeply with increasing $|\Delta y|$ or $\Delta\varphi$ varying from $\Delta\varphi = \pi$ down to zero. Therefore, an overshoot of experimentally-observed cross-section over best available SPS predictions in the region $\Delta\varphi \rightarrow 0$ or $|\Delta y| \gg 1$ can be interpreted as a signature of DPS.

Another way to probe the DPS mechanism is to use the fact that due to Eq. (1) the DPS cross-section grows with energy roughly as a square of SPS cross-section, so at sufficiently high energy the power-suppression by hard scale will be compensated by quickly growing

cross-section and the DPS contribution will dominate. To observe this effect at available energies, one chooses the process, for which SPS cross-section is as small as possible, due to suppression by high power of α_s . The hard scale also should be small in comparison to the collision energy, so that one stays in the low- x region, where Eq. (1) is applicable. Pair production of mesons containing c and b quarks seems to be an ideal playground for this kind of studies. But one has to anticipate, that due to low hard scales and involvement of relatively poorly understood physics of hadronization, the SPS cross-section could receive unexpectedly large higher-order QCD corrections, which could invalidate the assumption of negligibility of the SPS contribution. Moreover, at low- x plenty of phase space is available for emission of additional relatively hard partons, which will broaden the distributions in variables like $\Delta\varphi$ and Δy , thus mimicking the effects of DPS and making the extraction of the DPS signal from differential distributions more model-dependent.

In Ref. [5] the strategy described in previous paragraph has been applied by LHCb-Collaboration for the search of DPS contribution in the process of associated production of prompt bottomonium $\Upsilon(1S)$ and open-charm mesons D^0 or D^+ in forward-rapidity region in pp -collisions with center-of-mass energies $\sqrt{S} = 7$ and 8 TeV at the Large Hadron Collider. The leading order (LO, $O(\alpha_s^4)$ in this case) calculations in Collinear Parton Model [6, 7] and Color-Singlet approximation for the hadronization of $b\bar{b} \rightarrow \Upsilon$ lead to a very small SPS total cross-section of this process, compared with the cross-section of inclusive production of Υ -mesons, calculated in a same approximation: $R_{\text{SPS}}^{(\text{LO})} = \sigma_{\text{SPS}}^{(\text{LO}, \text{CS})}(\Upsilon + c\bar{c})/\sigma_{\text{SPS}}^{(\text{LO}, \text{CS})}(\Upsilon) = (0.2 - 0.6)\%$, while experimentally this ratio reaches almost 8% at $\sqrt{S} = 8$ TeV [5]. Such a large discrepancy was interpreted in Ref. [5] as a clear signal of DPS mechanism. This interpretation was supported by the fact, that shapes of differential distributions measured in Ref. [5] can be reasonably described by simple Monte-Carlo calculations based on measured inclusive cross-sections of production of Υ and D -mesons and “pocket-formula” (1).

In the present paper we reconsider the estimation of SPS contribution to above-described process, adding a few effects which were missed in calculations of Refs. [6, 7]. First, we approximately take into account higher-order corrections coming from Initial-State Radiation (ISR) effects, by virtue of Parton Reggeization Approach (PRA) [8, 9], which allows to factorize most significant part of ISR corrections into unintegrated Parton Distribution Functions (unPDFs) consistently with QCD gauge-invariance. The latter fact allows us to take into account the contributions to the $b\bar{b} \rightarrow \Upsilon$ coming from color-octet $b\bar{b}$ -pair in a

framework of nonrelativistic QCD (NRQCD) factorization approach [10]. An importance of color-octet contributions for bottomonium production in PRA has been demonstrated by us in Ref. [11]. And finally, we consistently take into account parton to D -meson hadronization, using the scale-dependent fragmentation functions, obtained in a global analysis of open-charm hadron production in e^+e^- -annihilation in Ref. [12]. Counter-intuitively, not only $c \rightarrow D$ but also $g \rightarrow D$ fragmentation plays an important role in the associated Υ and D production. Gluon fragmentation has also been found to be important for the same-sign DD -pair production in Refs. [13, 14]. In total and taking into account the uncertainties, our hybrid PRA+NRQCD+fragmentation model can account more than a half of experimentally observed cross-section for ΥD pair production. The shapes of all differential distributions in our SPS model also turn out to reproduce experimental data rather well, except for the shape of $\Delta\varphi$ -spectrum which has a puzzling “upside-down” behavior, un-explainable even by the DPS model (1). Therefore, we show that radiative corrections to the SPS cross-section of the process under consideration are large and mimicking the behavior of DPS, thus weakening the case for DPS-dominance in this process.

The paper is organized as follows. We describe the basics of PRA in the Sec. II. In the Sec. III we present our model of $\Upsilon(1S)D^{0,+}$ pair production. Then we concentrate on the numerical results and comparison with experimental data of the Ref. [5] in the Sec. IV. Finally, we summarize our conclusions in the Sec. V.

II. PARTON REGGEIZATION APPROACH

The brief description of LO approximation of PRA is presented below. More details can be found in Ref. [9], the development of PRA in the next-to-leading order (NLO) approximation is further discussed in [15, 16]. The main ingredients of PRA are k_T -dependent factorization formula, unintegrated parton distribution functions (unPDF’s) and gauge-invariant amplitudes with off-shell initial-state partons, derived using the Lipatov’s Effective Field Theory (EFT) of Reggeized gluons [17] and Reggeized quarks [18].

Factorization formula of PRA in LO approximation for the process $p+p \rightarrow \mathcal{Y}+X$, can be obtained from factorization formula of the CPM for the auxiliary hard subprocess $g+g \rightarrow g+\mathcal{Y}+g$. In the Ref. [9] the modified Multi-Regge Kinematics (mMRK) approximation for the auxiliary amplitude is constructed, which correctly reproduces the Multi-Regge and

collinear limits of corresponding QCD amplitude. This mMRK-amplitude has t -channel factorized form, which allows one to rewrite the cross-section of auxiliary subprocess in a k_T -factorized form:

$$d\sigma = \int_0^1 \frac{dx_1}{x_1} \int \frac{d^2\mathbf{q}_{T1}}{\pi} \tilde{\Phi}_g(x_1, t_1, \mu^2) \int_0^1 \frac{dx_2}{x_2} \int \frac{d^2\mathbf{q}_{T2}}{\pi} \tilde{\Phi}_g(x_2, t_2, \mu^2) \cdot d\hat{\sigma}_{\text{PRA}}, \quad (2)$$

where $t_{1,2} = -\mathbf{q}_{T1,2}^2$, the off-shell partonic cross-section $\hat{\sigma}_{\text{PRA}}$ in PRA is determined by squared PRA amplitude, $|\overline{\mathcal{A}_{\text{PRA}}}|^2$. Despite the fact that four-momenta $(q_{1,2})$ of partons in the initial state of amplitude \mathcal{A}_{PRA} are off-shell ($q_{1,2}^2 = -t_{1,2} < 0$), the PRA hard-scattering amplitude is *gauge-invariant* because the initial-state off-shell gluons are treated as Reggeized gluons (R) in a sense of gauge-invariant EFT for QCD processes in Multi-Regge Kinematics(MRK), introduced by L.N. Lipatov in [17]. The Feynman rules of this EFT are written down in Ref. [19].

The tree-level "unintegrated PDFs" (unPDFs) $\tilde{\Phi}_g(x_{1,2}, t_{1,2}, \mu^2)$ in Eq. (2) are equal to the convolution of the collinear PDF $f_g(x, \mu^2)$ and Dokshitzer-Gribov-Lipatov-Altarelli-Parisi (DGLAP) splitting function $P_{gg}(z)$ with the factor $1/t_{1,2}$. Consequently, the cross-section (2) with such unPDFs contains the collinear divergence at $t_{1,2} \rightarrow 0$ and infrared (IR) divergence at $z_{1,2} \rightarrow 1$. To regularize the latter, we observe, that the mMRK expression gives a reasonable approximation for the exact matrix element only in the rapidity-ordered part of the phase-space $y_{g_1} > y_g > y_{g_2}$. From this requirement, the following cutoff on $z_{1,2}$ can be derived: $z_{1,2} < 1 - \Delta_{\text{KMR}}(t_{1,2}, \mu^2)$, where $\Delta_{\text{KMR}}(t, \mu^2) = \sqrt{t}/(\sqrt{\mu^2} + \sqrt{t})$ is the Kimber-Martin-Ryskin (KMR) cutoff function [20], and we have taken into account that $\mu^2 \sim M_{T\gamma}^2$. The collinear singularity at $t_{1,2} \rightarrow 0$ is regularized by the Sudakov formfactor:

$$T_i(t, \mu^2) = \exp \left[- \int_t^{\mu^2} \frac{dt'}{t'} \frac{\alpha_s(t')}{2\pi} \sum_{j=q,\bar{q},g} \int_0^1 dz z \cdot P_{ji}(z) \theta \left(1 - \Delta_{\text{KMR}}(t', \mu^2) - z \right) \right], \quad (3)$$

which resums doubly-logarithmic corrections $\sim \log^2(t/\mu^2)$ in the Leading-Logarithmic-Approximation.

The final form of our unPDF in PRA is:

$$\Phi_i(x, t, \mu^2) = \frac{T_i(t, \mu^2)}{t} \frac{\alpha_s(t)}{2\pi} \sum_{j=q,\bar{q},g} \int_x^1 dz P_{ij}(z) \cdot \frac{x}{z} f_j \left(\frac{x}{z}, t \right) \cdot \theta \left(1 - \Delta_{\text{KMR}}(t, \mu^2) - z \right), \quad (4)$$

which coincides with Kimber, Martin and Ryskin unPDF [20]. The KMR unPDF is actively used in the phenomenological studies employing k_T -factorization, but to our knowledge, the

derivation, presented in [9] is the first systematic attempt to clarify its relationships with MRK limit of the QCD amplitudes.

In contrast to most of studies in the k_T -factorization, the gauge-invariant matrix elements with off-shell initial-state partons (Reggeized quarks and gluons) from Lipatov's EFT [17, 18] allow one to study arbitrary processes involving non-Abelian structure of QCD without violation of Slavnov-Taylor identities due to the nonzero virtuality of initial-state partons. This approach, together with KMR unPDFs gives stable and consistent results in a wide range of phenomenological applications, which include the description of the angular correlations of dijets [8], b -jets [21], charmed [14] and bottom-flavored [9] mesons, as well as some other examples.

A few years ago, the new approach to derive gauge-invariant scattering amplitudes with off-shell initial-state partons for high-energy scattering, using the spinor-helicity techniques and BCFW-like recursion relations for such amplitudes has been introduced in the Refs. [22–24]. This formalism for numerical generation of off-shell amplitudes is equivalent to the Lipatov's EFT at the tree level, but for some observables, e. g. related with production of heavy quarkonia, or for the generalization of the formalism to NLO [15, 16], the use of explicit Feynman rules and the structure of EFT is more convenient.

III. MODEL FOR ΥD PAIR PRODUCTION

In the Leading Order (LO), ($O(\alpha_s^3)$), in PRA plus fragmentation model [25], only gluon fragmentation contributes to the process of associated production of bottomonium and D -meson:

$$R + R \rightarrow \Upsilon(3S, 2S, 1S) + g(\rightarrow D), \quad (5)$$

$$R + R \rightarrow \chi_b(2P, 1P) + g(\rightarrow D). \quad (6)$$

One might worry, that the gain of one power of α_s will be compensated by small numerical value of $g \rightarrow D$ fragmentation function in comparison with $c \rightarrow D$ fragmentation and thus the numerically leading contribution comes from the Next-to-Leading-Order (NLO) ($O(\alpha_s^4)$) subprocesses:

$$R + R \rightarrow \Upsilon(3S, 2S, 1S) + c(\rightarrow D) + \bar{c}, \quad (7)$$

$$R + R \rightarrow \chi_b(2P, 1P) + c(\rightarrow D) + \bar{c}. \quad (8)$$

We address this question in Sec. IV and show, that contribution of $2 \rightarrow 3$ subprocesses is actually subleading, so in the final predictions for the cross-sections and spectra we take into account only subprocesses (5, 6).

According to NRQCD factorization formalism [10], final heavy quarkonium can be produced via color-singlet and color-octet intermediate states of $b\bar{b}$ -pair. We use the set of color-singlet and color-octet nonperturbative (long-distance) matrix elements (NMEs or LDMEs), which has been obtained in the LO PRA plus NRQCD-factorization approximation in the Ref. [11] from the fit of inclusive p_T -spectra of prompt $\Upsilon(nS)$ -mesons, measured by ATLAS, CMS and LHCb Collaborations at the LHC. For reader's convenience, we collect these NMEs in the Table I. The color-octet contributions for the production of P -wave bottomonia tend to be negligible in comparison with color-singlet contributions [11], so in the P -wave case we take into account only the singlet channel. Thus at the quark level we are left with the following list of LO partonic subprocesses:

$$R + R \rightarrow b\bar{b}[{}^3S_1^{(1)}] + g, \quad (9)$$

$$R + R \rightarrow b\bar{b}[{}^3S_1^{(8)}] + g, \quad (10)$$

$$R + R \rightarrow b\bar{b}[{}^3P_{0,1,2}^{(1)}] + g. \quad (11)$$

The sets of Feynman diagrams of Lipatov's EFT which describe subprocesses (9-11) are shown in Fig. 1. Squared off-shell amplitude of subprocess (9) is well known, it was calculated many years ago in the Ref. [27]. Squared off-shell amplitudes of subprocess (10) and (11) are calculated here for the first time. However, corresponding on-shell squared amplitudes are known [28] and they have been used for the test of collinear limit of obtained PRA amplitudes with off-shell initial-state partons. To automatize the analytic calculations we have implemented the Feynman rules of EFT [17, 18] as a model for FeynArts package [29]. The further calculation of helicity amplitudes for $2 \rightarrow 2$ and $2 \rightarrow 3$ processes has been performed using FeynCalc [30] package and for the numerical evaluation, amplitudes had been squared, summed over colors and helicities and implemented as a FORTRAN code. Unfortunately, due to complicated dependence on light-cone and transverse components of four-momenta of initial and final-state particles, PRA amplitudes even for $2 \rightarrow 2$ processes tend to become prohibitively large for the journal publication. In fact, in the case of ${}^3S_1^{(8)}$ -subprocess (10) the arithmetic with quadruple precision inside the squared-amplitude routine is required to reach numerical stability of the calculation.

Considering the associated production of $\Upsilon(1S)D^{0,+}$ pairs, one should take into account both direct and feed-down production of $\Upsilon(1S)$ via decays of higher-lying $\Upsilon(3S, 2S)$ and $\chi_b(2P, 1P)$ states, which in turn are produced directly or via decays of even excited states. Taking known branching fractions of different decays from [31] and considering cascades of up to three consequent decays we have obtained the following cascade branching fractions for $\Upsilon(1S)$ -state: $\text{Br}(\Upsilon(3S) \rightarrow \Upsilon(1S)) = 0.138$, $\text{Br}(\chi_{b2}(2P) \rightarrow \Upsilon(1S)) = 0.114$, $\text{Br}(\chi_{b1}(2P) \rightarrow \Upsilon(1S)) = 0.171$, $\text{Br}(\chi_{b0}(2P) \rightarrow \Upsilon(1S)) = 0.023$, $\text{Br}(\Upsilon(2S) \rightarrow \Upsilon(1S)) = 0.302$, $\text{Br}(\chi_{b2}(1P) \rightarrow \Upsilon(1S)) = 0.191$, $\text{Br}(\chi_{b1}(1P) \rightarrow \Upsilon(1S)) = 0.339$, $\text{Br}(\chi_{b0}(1P) \rightarrow \Upsilon(1S)) = 0.018$, which are used in the calculation.

To describe the D -meson production we use the fragmentation model in which the transition of gluon to the D meson is described by corresponding scale-dependent fragmentation function (FF) $D_g(z, \mu^2)$ [25]. Recently, the non-trivial role of gluon fragmentation in associated production of same-sign D -meson pairs at the LHC has been demonstrated by some of us [14]. The latter process has been considered by some authors as clean signal of DPS production mechanism [26]. In Ref. [14] it has been shown that main mechanism of same-sign DD -pair production is gluon to D meson fragmentation via production of gluon pair in the LO PRA subprocess $RR \rightarrow gg$. The description of LHCb data [32] has been archived without hypothesis on large DPS contribution. In the present paper, as well as in the Ref. [14] we use universal scale-dependent LO FFs of the Ref. [12], fitted to e^+e^- -annihilation data from CERN LEP1.

IV. RESULTS AND DISCUSSION

Here we discuss our numerical results obtained for prompt $\Upsilon(1S)D^{0,+}$ pair production in pp -collisions at energies $\sqrt{S} = 7$ TeV and $\sqrt{S} = 8$ TeV. We use the unPDFs obtained by the KMR formula (3, 4) from the LO collinear PDFs MSTW-2008 [33] and the corresponding value of $\alpha_s(M_Z) = 0.13939$. We set the renormalization and factorization scales to $\mu_R = \mu_F = \frac{\xi}{2} \left(\sqrt{M_\Upsilon^2 + p_{T\Upsilon}^2} + \sqrt{M_D^2 + p_{TD}^2} \right)$ where $\xi = 1$ for the central lines of our predictions, and we vary $1/2 < \xi < 2$ to estimate the scale-uncertainty of our prediction, which is shown in the figures by the gray band for the curve corresponding to the sum of all contributions.

In the Figs. 2 and 5, we compare normalized transverse momentum and rapidity spectra of $\Upsilon(1S)$ and $D^{0,+}$ predicted by our model with LHCb data [5]. The top panels of Figs. 3

and 6 collect rapidity and transverse momentum spectra of $\Upsilon(1S)D^{0,+}$ pairs. For all above-mentioned spectra, our hybrid LO PRA plus NRQCD plus fragmentation model does reasonably well in explaining the experimental data.

At the bottom panels of Figs. 3 and 6 we plot spectra for the rapidity difference $\Delta y = |y_{\Upsilon} - y_D|$ and for the azimuthal angle difference $\Delta\varphi = |\varphi_{\Upsilon} - \varphi_D|$. The Δy spectra are reasonably well described. The $\Delta\varphi$ spectrum obtained in our model has typical shape for this kind of spectra. It has one peak at the $\Delta\varphi \rightarrow \pi$ and plateau at the $\Delta\varphi \leq \pi/2$. However, the experimental data from LHCb Collaboration, though having large errors, demonstrate existence of the second peak for $\Delta\varphi \rightarrow 0$. This feature of the data can not be explained even by the DPS-model based on Eq. (1), which predicts the flat, un-correlated $\Delta\varphi$ -spectrum.

In the Figs. 4 and 7, we plot spectra for the invariant mass of $\Upsilon(1S)D^{0,+}$ pair (M) and transverse momentum asymmetry $A_T = (p_{T\Upsilon} - p_{TD})/(p_{T\Upsilon} + p_{TD})$. Predictions of our model with this correlation spectra also agree reasonably well with LHCb data.

Now we turn to the discussion of predictions of our SPS model for total cross-sections $B_{\mu^+\mu^-} \times \sigma^{\Upsilon D^{0,+}}$ (where $\Upsilon(1S) \rightarrow \mu^+\mu^-$ branching fraction $B_{\mu^+\mu^-} = 0.025$ is taken into account). At $\sqrt{S} = 7$ TeV, central values of our predictions for $\Upsilon(1S)D^0$ and $\Upsilon(1S)D^+$ production are 91 pb and 36 pb respectively (Tab. II) which, especially taking into account large scale-uncertainty, reaches almost more than one half of the experimental cross-section, which is respectively 155 and 82 pb. Different contributions to the total cross section and its scale-uncertainty are presented in Tables II and III, correspondingly for the energies $\sqrt{S} = 7$ TeV and $\sqrt{S} = 8$ TeV. Feed-down contribution from decays of higher lying bottomonium states ($\Upsilon(3S), \Upsilon(2S), \chi_b(2P), \chi_b(1P)$) is not small, it is about 50% from total calculated cross section. Contribution of color-singlet processes (5) and (6) is always dominant, but contribution of $[^3S_1^{(8)}]$ intermediate state is also very important, reaching up to a half of the $[^3S_1^{(1)}]$ intermediate state contribution.

In our model, the main source of $D^{0,+}$ mesons is the gluon fragmentation. Let's compare above results with the model based on c -quark fragmentation into D mesons. We have calculated direct production cross sections via color-singlet and color-octet intermediate states in process (7) which on the quark level corresponds to

$$R + R \rightarrow b\bar{b}[^3S_1^{(1,8)}] + c + \bar{c}. \quad (12)$$

Due to fragmentation model, we have to take the c -quark as massless, however we take

into account threshold condition for invariant mass of $c\bar{c}$ -pair: $s_{c\bar{c}} = (p_c + p_{\bar{c}})^2 > 4m_c^2$ with $m_c = 1.5$ GeV. Our $2 \rightarrow 3$ amplitudes passed numerous cross-checks, in particular, we have numerically checked, that *final-state collinear* limit ($s_{c\bar{c}} \ll \min(p_{Tc}^2, p_{T\bar{c}}^2)$) of the squared amplitudes of the processes (12) is related with the squared amplitudes of the processes (9, 10) by the well-known collinear-factorization relation for tree-level amplitudes:

$$\langle |\overline{\mathcal{M}[RR \rightarrow b\bar{b} + c(p_c) + \bar{c}(p_{\bar{c}})]}|^2 \rangle \simeq \frac{2g_s^2}{s_{c\bar{c}}} P_{qg}(z) \cdot \overline{|\mathcal{M}[RR \rightarrow b\bar{b} + g(p_c + p_{\bar{c}})]|^2},$$

where $z = p_c^0/(p_c^0 + p_{\bar{c}}^0)$, $P_{qg}(z) = [z^2 + (1-z)^2]/2$ and angular brackets in the l.h.s. stand for the averaging over azimuthal angle parametrizing the directions of momenta \mathbf{p}_c and $\mathbf{p}_{\bar{c}}$ for constant $\mathbf{p}_c + \mathbf{p}_{\bar{c}}$ and z .

For the direct contributions from the subprocesses (12) we obtain $B_{\mu^+\mu^-} \times \sigma_{\text{direct}}^{D^0}[R+R \rightarrow b\bar{b}[{}^3S_1^{(1+8)}] + c + \bar{c}] = 20$ pb at $\sqrt{S} = 7$ TeV and 24 pb at $\sqrt{S} = 8$ TeV, so for ratio of direct cross sections we obtain:

$$\frac{\sigma_{\text{direct}}^{D^0}[R+R \rightarrow b\bar{b}[{}^3S_1^{(1+8)}] + g]}{\sigma_{\text{direct}}^{D^0}[R+R \rightarrow b\bar{b}[{}^3S_1^{(1+8)}] + c + \bar{c}]} \simeq 2.6 \div 2.5,$$

at $\sqrt{S} = 7$ and 8 TeV. So our expectation of the dominant role of the gluon fragmentation in this process turns out to be correct.

V. CONCLUSIONS

In the present paper we have demonstrated, that conclusion about DPS-dominance in the total cross-section for the process of associated hadroproduction of Υ and D mesons, based on the LO CPM calculations of Refs. [6, 7] was premature and one can relatively easily come up with the model which accounts more than a half of the observed cross-section. Also, due to the use of High-Energy factorization with unPDFs dependent on transverse momenta of initial-state partons, the leading part of ISR corrections has been taken into account and all differential distributions are described reasonably well. Therefore one have to be rather careful about the statements that DPS dominates total cross-section of relatively low-scale, hadronization-sensitive processes like one considered in the present paper. Most likely, the solid evidence in favor of DPS can be obtained only from studies of differential distributions in specific regions of phase space and at high scales, where radiative corrections to SPS contribution can be put under theoretical control.

Acknowledgments

Authors thank the Ministry of Education and Science of the Russian Federation for financial support in the framework of the Samara University Competitiveness Improvement Program among the world's leading research and educational centers for 2013-2020, the task No 3.5093.2017/8.9 and the Foundation for the Advancement of Theoretical Physics and Mathematics BASIS, grant No. 18-1-1-30-1. We thank Prof. B.A. Kniehl and Dr. Zhi-Guo He for stimulating discussions.

-
- [1] M. Diehl, J. R. Gaunt, P. Plöthl and A. Schafer. Two-loop splitting in double parton distributions, arXiv:1902.08019 [hep-ph].
- [2] M. Diehl and R. Nagar. Factorisation of soft gluons in multiparton scattering, arXiv:1812.09509 [hep-ph].
- [3] M. Diehl, D. Ostermeier and A. Schafer. Elements of a theory for multiparton interactions in QCD, JHEP **1203** (2012) 089 Erratum: [JHEP **1603** (2016) 001] doi:10.1007/JHEP03(2012)089, 10.1007/JHEP03(2016)001
- [4] E. Elias, K. Golec-Biernat and A. M. Stasto. Numerical analysis of the unintegrated double gluon distribution, JHEP **1801** (2018) 141. doi:10.1007/JHEP01(2018)141
- [5] *Aaij R. et al.* [LHCb Collaboration]. Production of associated Υ and open pcharm hadrons in pp collisions at $\sqrt{S} = 7$ and 8 TeV via double parton scattering // JHEP **07** (2016) 052.
- [6] A.V. Berezhnoy, A.K. Likhoded. Associated production of Υ and open charm at LHC. Int.J.Mod.Phys. **A30** (2015) 1550125.
- [7] A.K. Likhoded, A.V. Luchinsky, S.V. Poslavsky. Production of associated χ_b and open charm at the LHC // Phys. Lett. **B755** (2016) 24.
- [8] M.A. Nefedov, V.A. Saleev, A.V. Shipilova Dijet azimuthal decorrelations at the LHC in the parton Reggeization approach, Phys. Rev. **D87** (2013) 094030.
- [9] M.A. Nefedov, A.V. Karpishkov, V.A. Saleev $B\bar{B}$ angular correlations at the LHC in the parton Reggeization approach merged with higher-order matrix elements // Phys. Rev. **D96** (2017) 096019.
- [10] G.T. Bodwin, E. Braaten, G.P. Lepage. Rigorous QCD analysis of inclusive annihilation and production of heavy quarkonium. Phys. Rev. **D51** (1995) 1125.
- [11] M.A. Nefedov, V.A. Saleev, A.V. Shipilova. Prompt $\Upsilon(nS)$ production at the LHC in the Regge limit of QCD. Phys. Rev. **D88** (2013) 014003.
- [12] B.A. Kniehl, G. Kramer, I. Schienbein, H. Spiesberger. Reconciling open-charm production at the Fermilab Tevatron with QCD. Phys. Rev. Lett. **96** (2006) 012001.
- [13] A. Karpishkov, V. Saleev, A. Shipilova A. Large-pT production of D mesons at the LHCb in the parton Reggeization approach. Phys. Rev. **D94** (2016) 114012.
- [14] R. Maciula, V.A. Saleev, A.V. Shipilova, A. Szczurek. New mechanisms for double charmed

- meson production at the LHCb // Phys. Lett. **B758** (2016) 458.
- [15] M.A. Nefedov, V.A. Saleev. On the one-loop calculations with Reggeized quarks, Mod. Phys. Lett. **A32** (2017) 1750207. M. A. Nefedov. Computing one-loop corrections to effective vertices with two scales in the EFT for Multi-Regge processes in QCD, arXiv:1902.11030 [hep-ph].
- [16] M.A. Nefedov, V.A. Saleev. From LO to NLO in the parton Reggeization approach EPJ Web Conf. 191 (2018) 04007.
- [17] L.N. Lipatov L.N. Gauge invariant effective action for high energy processes in QCD. Nucl. Phys. **B452** (1995) 369.
- [18] L.N. Lipatov, M.I. Vyazovsky. Quasi-multi-Regge processes with a quark exchange in the t-channel, Nucl. Phys. **B597** (2001) 399.
- [19] E.N. Antonov, L.N. Lipatov, E.A. Kuraev, I.O. Cherednikov. Feynman rules for effective Regge action, Nucl. Phys. **B721** (2005) 111.
- [20] M.A. Kimber, A.D. Martin, M.G. Ryskin. Unintegrated parton distributions, Phys. Rev. **D63** (2001) 114027.
- [21] V.A. Saleev, A.V. Shipilova. Inclusive b-jet and bb-dijet production at the LHC via Reggeized gluons, Phys. Rev. **D86** (2012) 034032.
- [22] A. van Hameren, P. Kotko, K. Kutak. Helicity amplitudes for high-energy scattering, JHEP **01** (2013) 078.
- [23] A. van Hameren, K. Kutak, T. Salwa. Scattering amplitudes with off-shell quarks, Phys. Lett. **B727** (2013) 226.
- [24] A. van Hameren, KaTie: For parton-level event generation with kT-dependent initial states, Comput.Phys.Comm. **224** (2018) 371.
- [25] B. Mele, P. Nason. The fragmentation function for heavy quarks in QCD, Nucl. Phys. **B361** (1991) 626.
- [26] M. Juszczak, R. Maciula, A. Szczurek. Production of two $c\bar{c}$ pairs in double-parton scattering, Phys. Rev. **D85** (2012) 094034.
- [27] B. A. Kniehl, D. V. Vasin, and V. A. Saleev, Charmonium production at high energy in the k(T)-factorization approach, Phys. Rev. **D73** (2006) 074022.
- [28] P. L. Cho and A. K. Leibovich. Color octet quarkonia production. 2, Phys. Rev. **D53** (1996) 6203; P. L. Cho and A. K. Leibovich, Color octet quarkonia production, Phys. Rev. **D53** (1996) 150.

- [29] T. Hahn. Generating Feynman diagrams and amplitudes with FeynArts 3, *Comput. Phys. Commun.* **140** (2001) 418.
- [30] R. Mertig, M. Bohm, A. Denner, FEYN CALC: Computer algebraic calculation of Feynman amplitudes, *Comput. Phys. Commun.* **64** (1991) 345.
- [31] C. Patrignani *et al.* [Particle Data Group]. Review of Particle Physics, *Chin. Phys.* **C40** (2016) 100001.
- [32] LHCb Collaboration, *Aaij R. et al.* [LHCb Collaboration]. Measurements of prompt charm production cross-sections in pp collisions at $\sqrt{S} = 13$ TeV // *JHEP* **03** (2016) 159.
- [33] A. D. Martin, W. J. Stirling, R. S. Thorne and G. Watt. Parton distributions for the LHC, *Eur. Phys. J.* **C63** (2009) 189.

TABLE I: The color-singlet and color-octet NMEs from Ref. [11] used in the calculation.

NME	Fit in LO PRA.
$\langle \mathcal{O}^{\Upsilon(1S)} [{}^3S_1^{(1)}] \rangle \times \text{GeV}^{-3}$	9.28
$\langle \mathcal{O}^{\Upsilon(1S)} [{}^3S_1^{(8)}] \rangle \times 10^2 \text{ GeV}^{-3}$	2.31 ± 0.25
$\langle \mathcal{O}^{\Upsilon(1S)} [{}^1S_0^{(8)}] \rangle \times 10^2 \text{ GeV}^{-3}$	0.0 ± 0.05
$\langle \mathcal{O}^{\Upsilon(1S)} [{}^3P_0^{(8)}] \rangle \times 10^2 \text{ GeV}^{-5}$	0.0 ± 0.38
$\langle \mathcal{O}^{\Upsilon(2S)} [{}^3S_1^{(1)}] \rangle \times \text{GeV}^{-3}$	4.62
$\langle \mathcal{O}^{\Upsilon(2S)} [{}^3S_1^{(8)}] \rangle \times 10^2 \text{ GeV}^{-3}$	1.51 ± 0.17
$\langle \mathcal{O}^{\Upsilon(2S)} [{}^1S_0^{(8)}] \rangle \times 10^2 \text{ GeV}^{-3}$	0.0 ± 0.01
$\langle \mathcal{O}^{\Upsilon(2S)} [{}^3P_0^{(8)}] \rangle \times 10^2 \text{ GeV}^{-5}$	0.0 ± 0.03
$\langle \mathcal{O}^{\Upsilon(3S)} [{}^3S_1^{(1)}] \rangle \times \text{GeV}^{-3}$	3.54
$\langle \mathcal{O}^{\Upsilon(3S)} [{}^3S_1^{(8)}] \rangle \times 10^2 \text{ GeV}^{-3}$	1.24 ± 0.13
$\langle \mathcal{O}^{\Upsilon(3S)} [{}^1S_0^{(8)}] \rangle \times 10^2 \text{ GeV}^{-3}$	0.0 ± 0.01
$\langle \mathcal{O}^{\Upsilon(3S)} [{}^3P_0^{(8)}] \rangle \times 10^2 \text{ GeV}^{-5}$	0.0 ± 0.02
$\langle \mathcal{O}^{\chi(1P)} [{}^3P_0^{(1)}] \rangle \times \text{GeV}^{-5}$	2.03
$\langle \mathcal{O}^{\chi(1P)} [{}^3S_1^{(8)}] \rangle \times 10^2 \text{ GeV}^{-3}$	0.0
$\langle \mathcal{O}^{\chi(2P)} [{}^3P_0^{(1)}] \rangle \times \text{GeV}^{-5}$	2.36
$\langle \mathcal{O}^{\chi(2P)} [{}^3S_1^{(8)}] \rangle \times 10^2 \text{ GeV}^{-3}$	0.0

TABLE II: The total cross sections of $\Upsilon D^{+,0}$ production at the LHCb for $\sqrt{S} = 7$ TeV.

	$B_{\mu^+\mu^-} \times \sigma^{\Upsilon(1S)D^0}$, pb	$B_{\mu^+\mu^-} \times \sigma^{\Upsilon(1S)D^+}$, pb
Direct contributions:	51	20
$R + R \rightarrow \Upsilon[{}^3S_1^{(1)}] + g$	37	15
$R + R \rightarrow \Upsilon[{}^3S_1^{(8)}] + g$	14	5
Sum of feed-down contributions (5), (6)	40	16
Total cross section, LO PRA	91_{-41}^{+48}	36_{-16}^{+19}
Total cross section, experiment [5]	155 ± 28	82 ± 24

TABLE III: The cross sections of $\Upsilon D^{+,0}$ production at the LHCb for $\sqrt{S} = 8$ TeV.

	$B_{\mu^+\mu^-} \times \sigma^{\Upsilon(1S)D^0}$, pb	$B_{\mu^+\mu^-} \times \sigma^{\Upsilon(1S)D^+}$, pb
Direct contributions:	61	24
$R + R \rightarrow \Upsilon[{}^3S_1^{(1)}] + g$	44	18
$R + R \rightarrow \Upsilon[{}^3S_1^{(8)}] + g$	17	6
Sum of feed-down contributions (5), (6)	49	19
Total cross section, LO PRA	108^{+56}_{-48}	42^{+22}_{-19}
Total cross section, experiment [5]	250 ± 39	80 ± 21

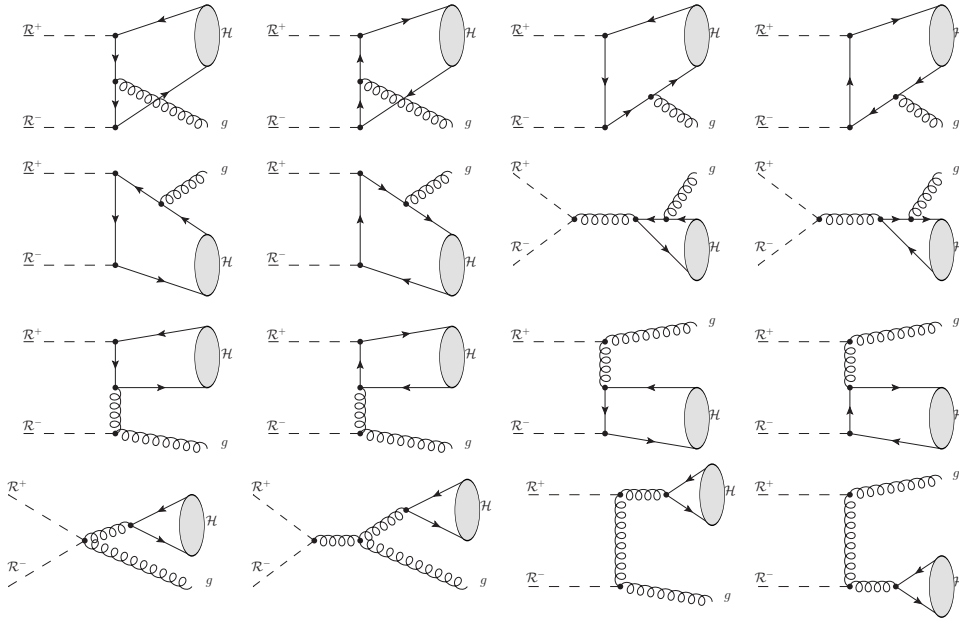


FIG. 1: Feynman diagrams used for direct production of S and P -wave bottomonia via color-singlet and color-octet intermediate states in processes $R + R \rightarrow b\bar{b}[{}^3S_1^{(1,8)}] + g$ and $R + R \rightarrow b\bar{b}[{}^3P_{0,1,2}^{(1)}] + g$.

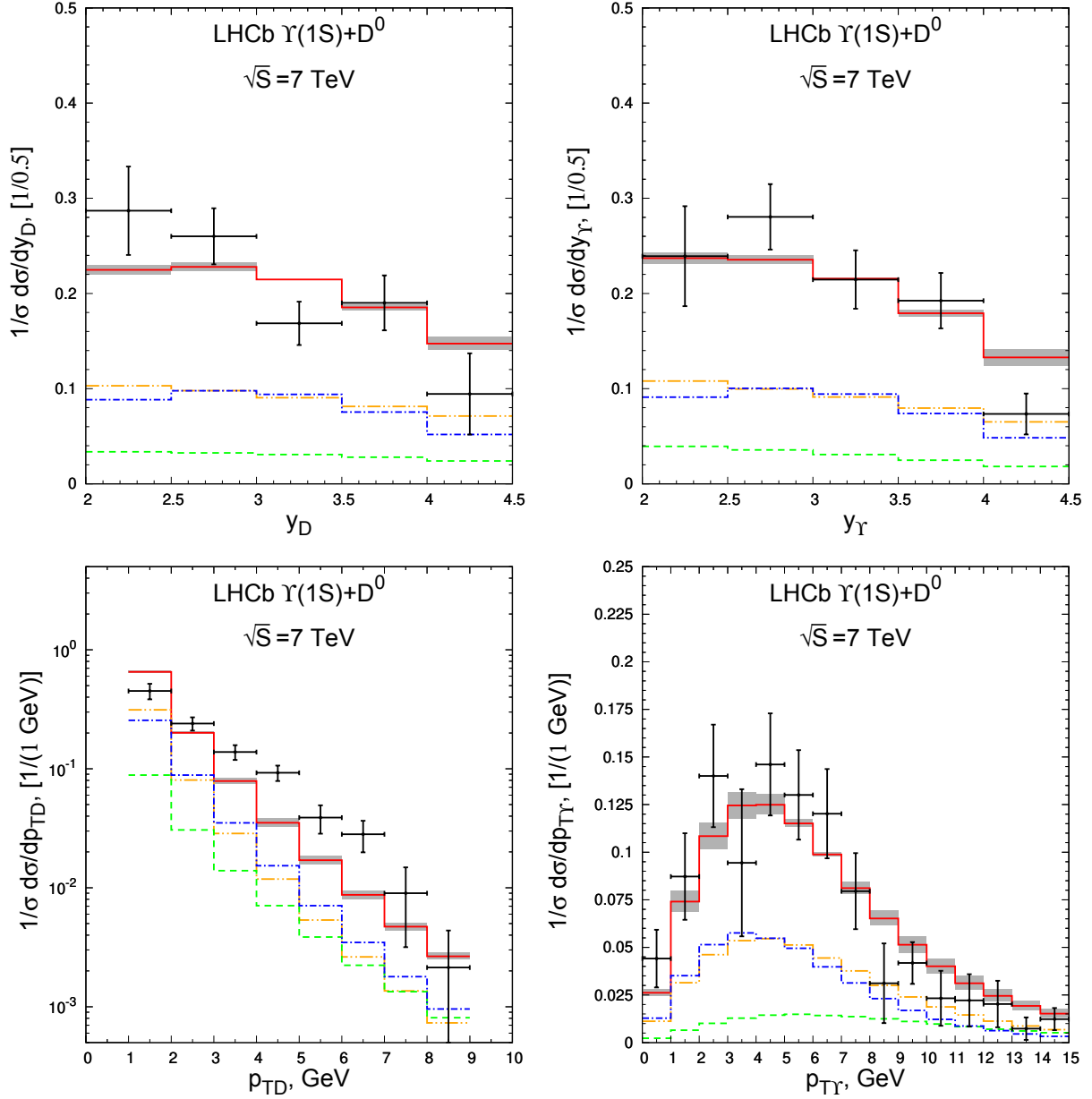


FIG. 2: Transverse momentum and rapidity spectra of $\Upsilon(1S)$ and D^0 . The LHCb data [5] are taken at $\sqrt{S} = 7$ TeV, $2.0 < y_{\Upsilon(D)} < 4.5$, $0 < p_{T\Upsilon} < 15$ GeV, and $1 < p_{TD} < 20$ GeV. Blue histograms are color-singlet contributions, green – color-octet contributions, orange – sum of feed-down contributions, red – sum of all contributions.

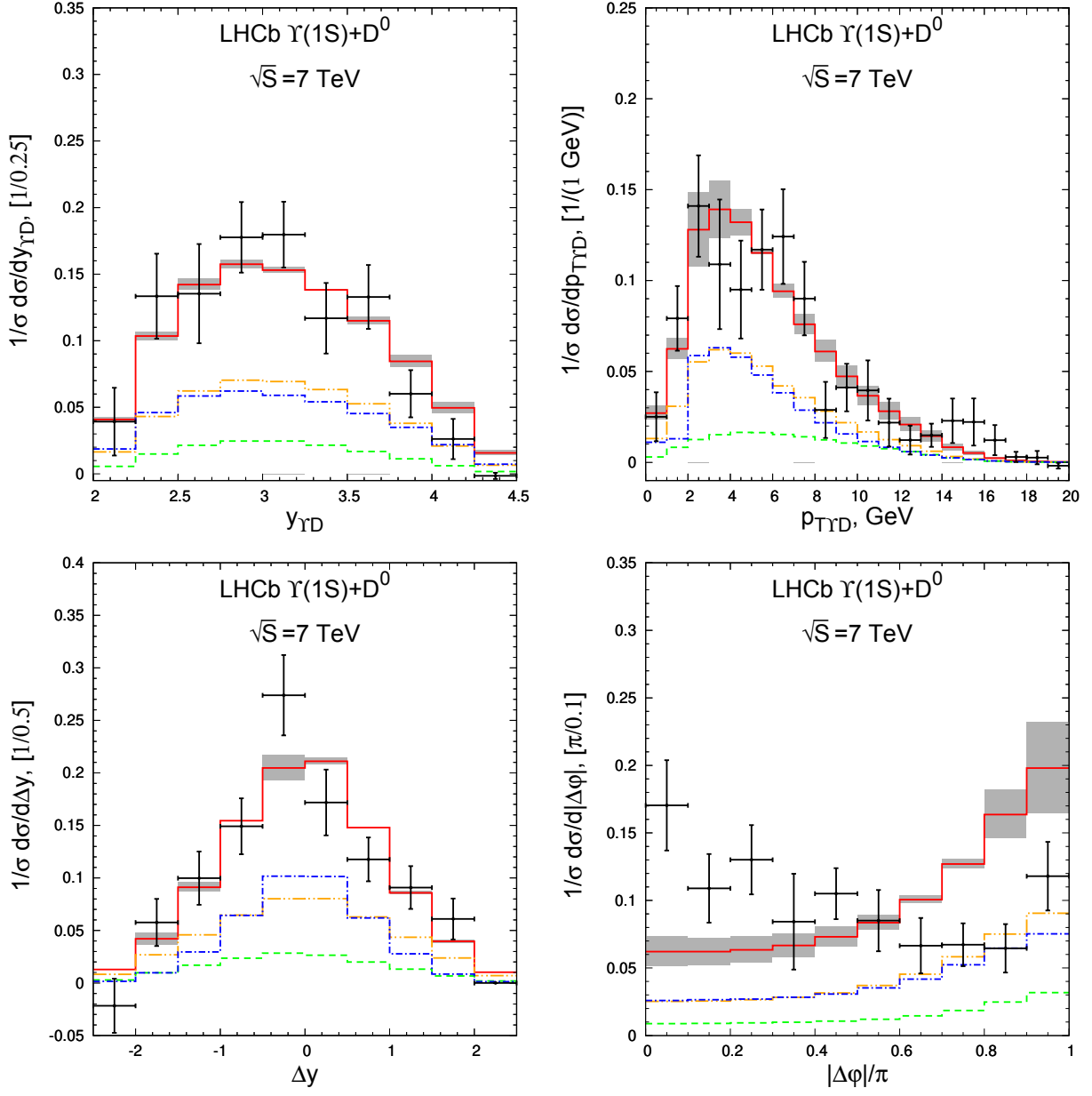


FIG. 3: Top panel: transverse momentum and rapidity spectra of $\Upsilon(1S)D^0$ pairs. Bottom panel: rapidity difference and azimuthal angle difference spectra. Histograms are the same as in the Fig. 2. The LHCb data [5] are taken at $\sqrt{S} = 7$ TeV, $2.0 < y_{\Upsilon(D)} < 4.5$, $0 < p_{T\Upsilon} < 15$ GeV, and $1 < p_{TD} < 20$ GeV.

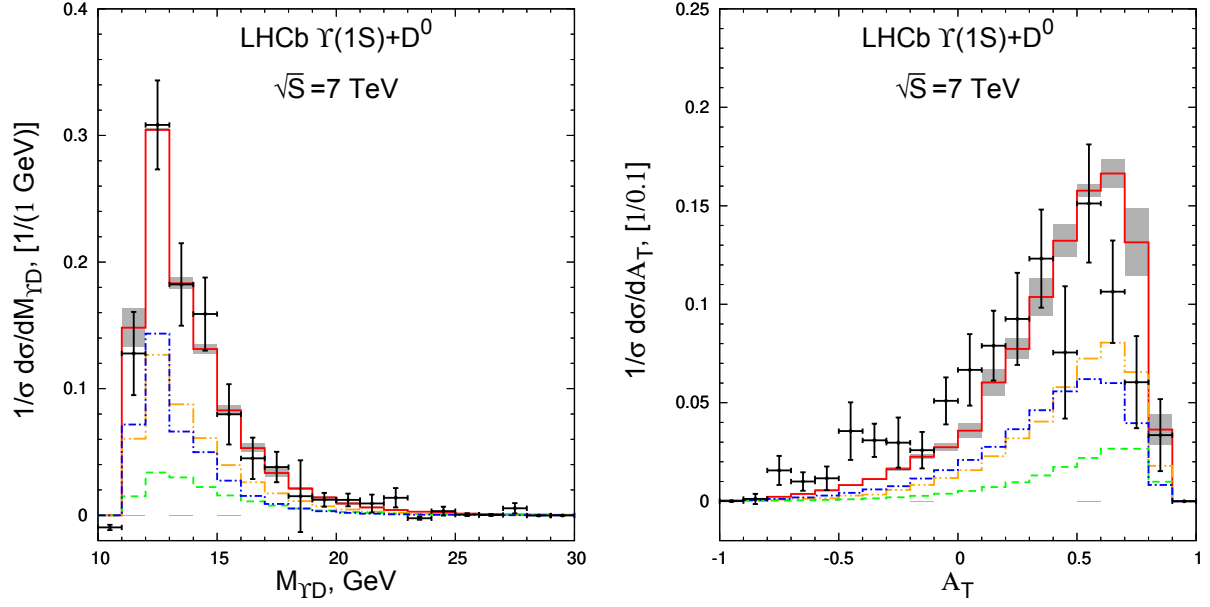


FIG. 4: Left panel: invariant mass spectrum of $\Upsilon(1S)D^0$ pairs. Right panel: transverse momentum asymmetry \mathcal{A}_T spectrum. Histograms are the same as in the Fig. 2. The LHCb data [5] are taken at $\sqrt{S} = 7$ TeV, $2.0 < y_{\Upsilon(D)} < 4.5$, $0 < p_{T\Upsilon} < 15$ GeV, and $1 < p_{TD} < 20$ GeV.

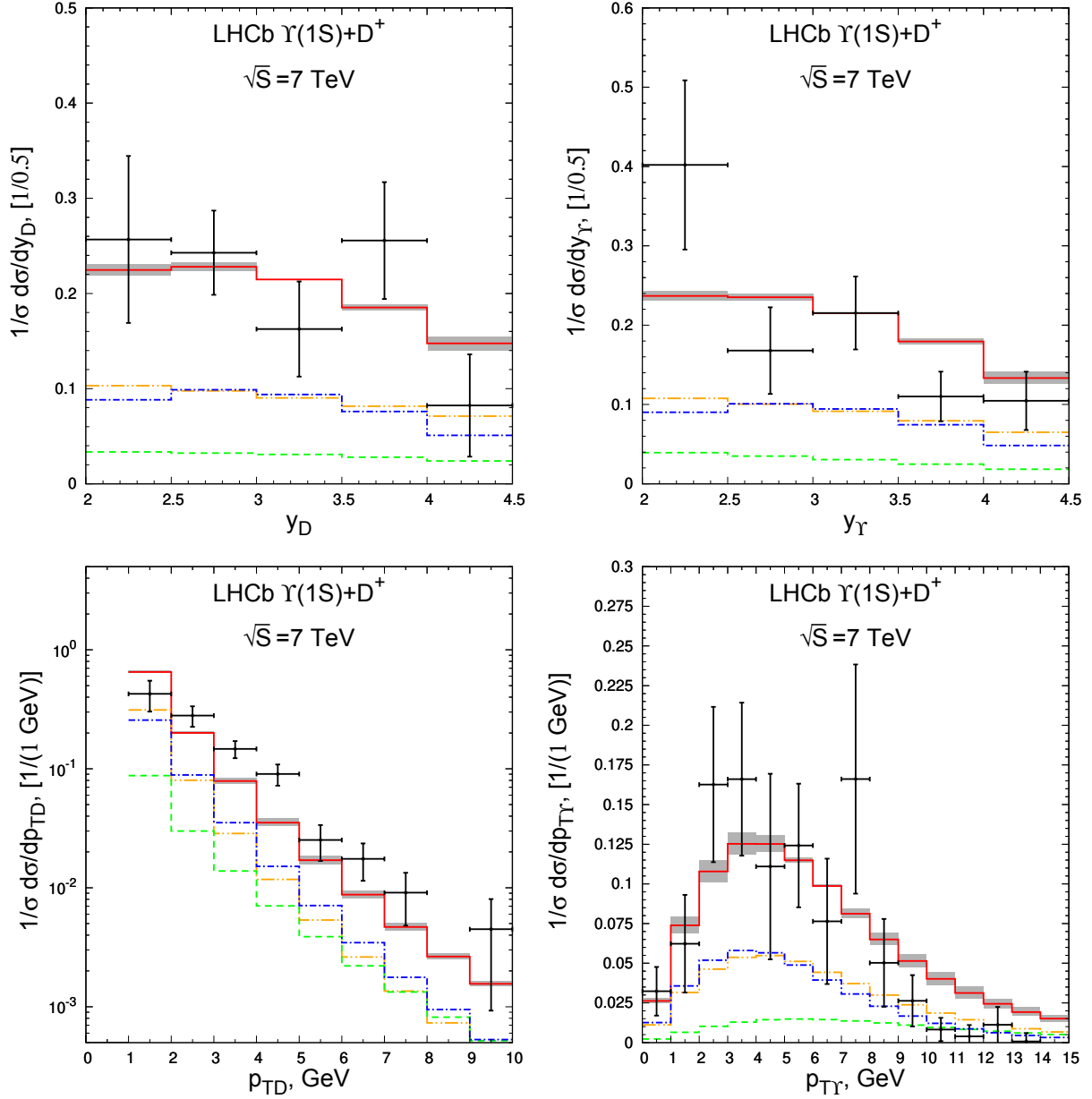


FIG. 5: Transverse momentum and rapidity spectra of $\Upsilon(1S)$ and D^+ . The LHCb data [5] are taken at $\sqrt{S} = 7$ TeV, $2.0 < y_{\Upsilon(D)} < 4.5$, $0 < p_{T\Upsilon} < 15$ GeV, and $1 < p_{TD} < 20$ GeV. Blue histograms are color-singlet contributions, green – color-octet contributions, orange – sum of feed-down contributions, red – sum of all contributions.

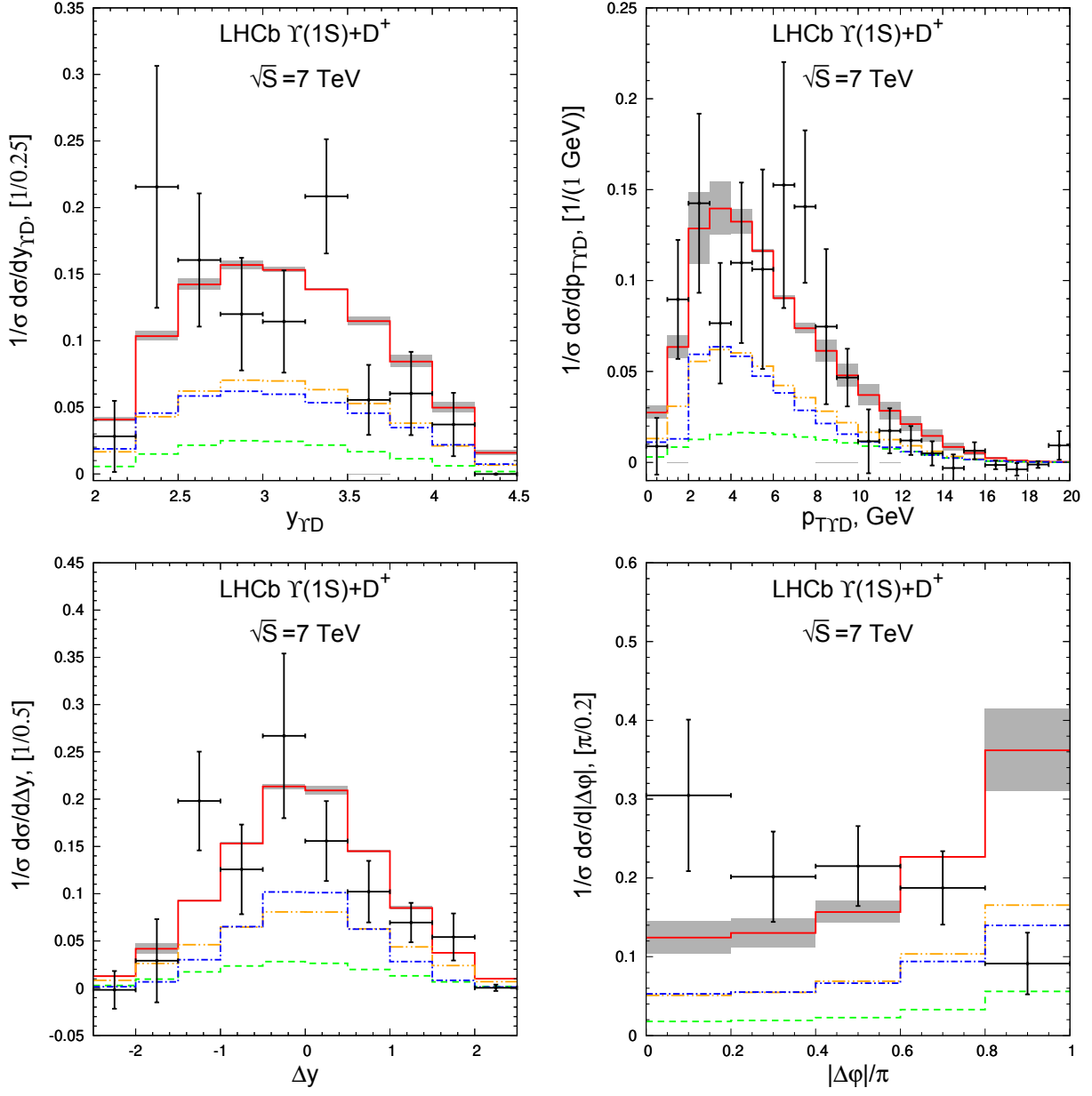


FIG. 6: Top panel: transverse momentum and rapidity spectra of $\Upsilon(1S)D^+$ pairs. Bottom panel: rapidity difference and azimuthal angle difference spectra. Histograms are the same as in the Fig. 2. The LHCb data [5] are taken at $\sqrt{S} = 7$ TeV, $2.0 < y_{\Upsilon(D)} < 4.5$, $0 < p_{T\Upsilon} < 15$ GeV, and $1 < p_{TD} < 20$ GeV.

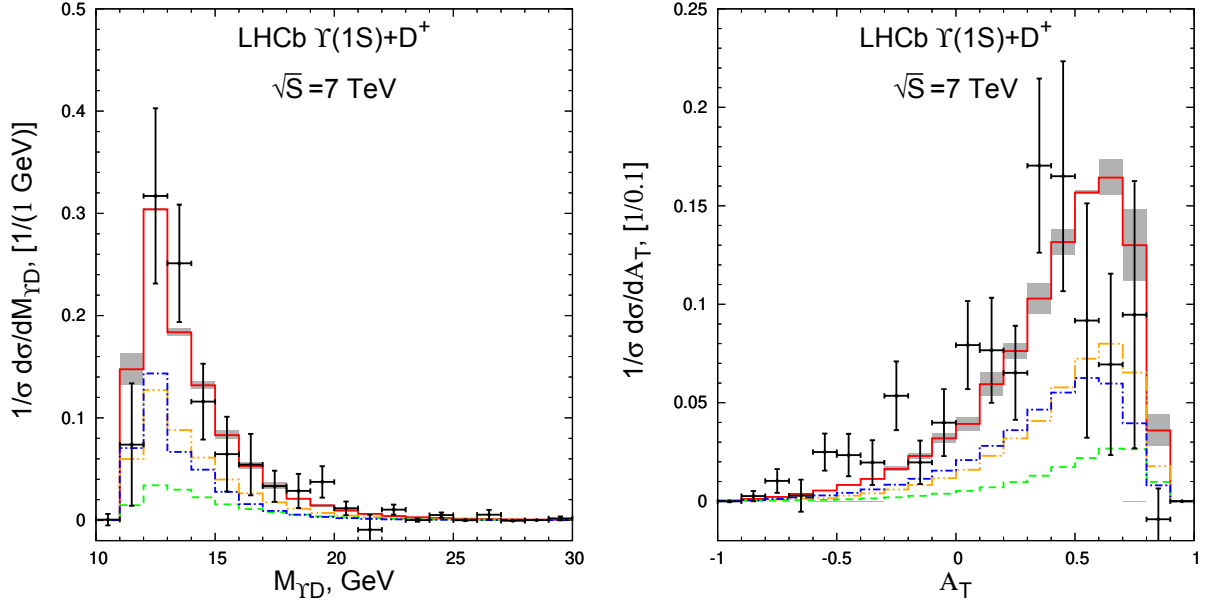


FIG. 7: Left panel: invariant mass spectrum of $\Upsilon(1S)D^+$ pairs. Right panel: transverse momentum asymmetry \mathcal{A}_T spectrum. Histograms are the same as in the Fig. 2. The LHCb data [5] are taken at $\sqrt{S} = 7$ TeV, $2.0 < y_{\Upsilon(D)} < 4.5$, $0 < p_{T\Upsilon} < 15$ GeV, and $1 < p_{TD} < 20$ GeV.